

Geodesic Motions in $2 + 1$ Dimensional Charged Black Holes

Dong Hyun Park* and Seung-ho Yang†

Department of Physics and Institute of Basic Science, Sungkyunkwan University

Suwon 440-746, Korea

Abstract

We study the geodesic motions of a test particle around $2 + 1$ dimensional charged black holes. We obtain a class of exact geodesic motions for the massless test particle when the ratio of its energy and angular momentum is given by square root of cosmological constant. The other geodesic motions for both massless and massive test particles are analyzed by use of numerical method.

PACS number(s): 04.20.jb, 04.25.Dm, 04.60.Kz, 04.70.Bw

Typeset using REVTeX

**E-mail address* : donghyun@newton.skku.ac.kr

†*E-mail address* : anka@newton.skku.ac.kr

I. INTRODUCTION

Since Bañados-Teitelboim-Zanelli(BTZ) reported the three dimensional black hole [1] as a series of solutions in $2 + 1$ dimensional anti-de Sitter gravity [2,3], it has become one of the most exciting problems in theoretical gravity. Black hole thermodynamics and statistical properties of BTZ black holes have been representative topics [4,5]. Recently the importance of BTZ-type black holes is emphasized because it has been demonstrated that the duality between gravity in $N + 1$ dimensional anti-de Sitter space and conformal field theory in N dimensions [6,7]. Among various branches of black hole researches, the simplest but basic topic is to investigate the classical geodesic motions in $2 + 1$ dimensional BTZ black holes. Though the exact solutions of geodesic motions were found for Schwarzschild- and Kerr-type BTZ black holes [8], no such solutions are known for a charged BTZ black hole. These aspects seem to be similar for the other research fields, e.g., black hole thermodynamics [4]. It has been believed by the following reason: The metric of a charged BTZ black hole involves both logarithm and the square of the radial coordinates. In this note, we found a class of exact geodesic motions for a charged BTZ black hole despite of the above obstacle. In addition, all other possible geodesic motions are categorized in examining the orbit equation, and analyzed by use of numerical method.

In next section, we briefly recapitulate charged BTZ black holes, and discuss the both null and time-like geodesics. We obtain a class of exact geodesic motions for the massless test particle when the ratio of its energy and angular momentum is given by square root of the absolute value of a negative cosmological constant. We conclude in Sec.III with a brief discussion.

II. GEODESIC MOTIONS

A static $2 + 1$ dimensional metric with rotational symmetry has the form;

$$ds^2 = B(r)e^{2N(r)}dt^2 - B^{-1}(r)dr^2 - r^2d\theta^2. \quad (1)$$

If there exists an electric point charge at the origin, the electrostatic field is given by $E_r = q/r$, and the diagonal components of energy-momentum tensor are non-vanishing, i.e., $T^t_t = T^r_r = -T^\theta_\theta = E_r^2/2e^{2N(r)}$. Then the Einstein equations become

$$\frac{1}{r} \frac{dN(r)}{dr} = 0, \quad (2)$$

$$\frac{1}{r} \frac{dB(r)}{dr} = 2|\Lambda| - \frac{8\pi Gq^2}{r^2 e^{2N(r)}}. \quad (3)$$

Static solutions of Eqs. (2) and (3) are

$$N(r) = N_0, \quad (4)$$

$$B(r) = |\Lambda|r^2 - 8\pi Gq^2 \ln r - 8GM, \quad (5)$$

where we have two integration constants N_0 and M . Note that the integration constant N_0 can be absorbed by rescaling of the time variable so that one can set it to be zero. The other constant M is identified by the mass of a BTZ black hole [9]. The obtained solutions are categorized into three classes characterized by the value of mass parameter M for a given value of charger q : (i) When $M < (\pi q^2/2) [1 - \ln(4\pi Gq^2/|\Lambda|)]$, the spatial manifold does not contain a horizon. (ii) When $M = (\pi q^2/2) [1 - \ln(4\pi Gq^2/|\Lambda|)]$, it has one horizon at $r = \sqrt{4\pi Gq^2/|\Lambda|}$ and then it corresponds to the extremal case of a charged BTZ black hole. (iii) When $M > (\pi q^2/2) [1 - \ln(4\pi Gq^2/|\Lambda|)]$, there are two horizons of a charged BTZ black hole.

Let us consider geodesic equations around the charged BTZ black hole. There are two constants of motions, γ and L , associated with two Killing vectors such as

$$B(r) \frac{dt}{ds} = \gamma, \quad (6)$$

$$r^2 \frac{d\theta}{ds} = L. \quad (7)$$

Geodesic equation for radial motions is read from the Lagrangian for a test particle:

$$B \left(\frac{dt}{ds} \right)^2 - \frac{1}{B} \left(\frac{dr}{ds} \right)^2 - r^2 \left(\frac{d\theta}{ds} \right)^2 = m^2 \quad (8)$$

where $m = 0$ stands for null (photon) geodesics and $m > 0$ time-like geodesics so that $m(> 0)$ sets to be 1 without loss of generality. Inserting Eqs. (6) and (7) into Eq. (8), we have a first-order equation

$$-\frac{1}{2} \left(\frac{dr}{ds} \right)^2 = -\frac{1}{2} \left\{ B(r) \left(\frac{L^2}{r^2} + m^2 \right) - \gamma^2 \right\}. \quad (9)$$

Then, all possible geodesic motions are classified by the shape of effective potential from the right-hand side of Eq. (9):

$$V(r) = \frac{1}{2} \left\{ B(r) \left(\frac{L^2}{r^2} + m^2 \right) - \gamma^2 \right\}. \quad (10)$$

From Eqs. (7) and (9), orbit equation is

$$\left(\frac{dr}{d\theta} \right)^2 = -B(r)r^2 \left(1 + \frac{m^2}{L^2}r^2 \right) + \frac{\gamma^2}{L^2}r^4. \quad (11)$$

From now on let us examine the orbit equation (11) and analyze all possible geodesic motions for various parameters. In the case of a photon without angular momentum ($m = 0$ and $L = 0$), the effective potential (10) becomes a constant:

$$V(r) = -\frac{\gamma^2}{2}. \quad (12)$$

For the regular case, all possible geodesic motions resemble those of a free particle. These solutions do not depend on both electric charge q and black hole mass M . For a black hole, the geodesic motions are similar to those of regular case far away from the horizon, however the existence of black hole horizons should be taken into account. Specifically the photon also has a free particle motion near the horizon, but the redshift is detected at the outside of black hole.

When a test photon carries angular momentum ($m = 0$ and $L \neq 0$), the effective potential (10) is

$$V(r) = \frac{1}{2} B(r) \left(\frac{L^2}{r^2} \right) - \frac{\gamma^2}{2}, \quad (13)$$

and the corresponding orbit equation is written as

$$d\theta = \frac{dr}{r\sqrt{4\pi Gq^2 \ln r^2 + 8MG + r^2\left(\frac{\gamma^2}{L^2} - |\Lambda|\right)}}. \quad (14)$$

There have been reported several well-known analytic solutions of geodesic equation for Schwarzschild- or Kerr-type BTZ black holes [8] because the orbit equations include the terms of the power of radial coordinates alone. Once we look at the form of the orbit equation in Eq. (14) with both the square of the radial coordinate and logarithmic terms, we may easily accept non-existence of analytic solutions of Eq. (14) when the electric charge q is nonzero. However, a clever but simple investigation shows an exit when $\gamma/L = \sqrt{|\Lambda|}$ in addition to the trivial Schwarzschild-type BTZ black hole in the limit of zero electric charge ($q = 0$): The coefficient of r^2 -term in the integrand vanishes and then a set of explicit orbits solution seems to exist. We will show that it is indeed the case.

As shown in FIGs. 1 and 2, all the geodesic motions of a photon in a charged BTZ black hole are categorized by five cases: (i) When $\gamma/L < (\gamma/L)_{\text{cr}}$, there is no allowed motion. Every orbit is allowed only when γ/L is equal to or larger than the critical value $(\gamma/L)_{\text{cr}}$:

$$\left(\frac{\gamma}{L}\right)_{\text{cr}} = \sqrt{|\Lambda| - \exp\left(\frac{2M}{\pi q^2} + \ln(4\pi Gq^2) - 1\right)}. \quad (15)$$

(ii) When $\gamma/L = (\gamma/L)_{\text{cr}}$, this condition gives a circular motion. The radius of this circular motion is

$$r_{\text{cir}} = \sqrt{\frac{4\pi Gq^2}{|\Lambda| - \left(\frac{\gamma}{L}\right)_{\text{cr}}^2}}. \quad (16)$$

Both critical value and radius of this circular motion are obtained from Eq. (13). (iii) When $(\gamma/L)_{\text{cr}} < \gamma/L < \sqrt{|\Lambda|}$, the photon has elliptic motions, but for the charged BTZ black hole with two horizon, the lower bound is limited by zero. (iv) When $\gamma/L = \sqrt{|\Lambda|}$, the geodesic equation becomes integrable. These geodesic motions are unbounded spiral motions at a large scale. (v) When $\gamma/L > \sqrt{|\Lambda|}$, the geodesic motions are unbounded. Note that for any charged BTZ black hole, $(\gamma/L)_{\text{cr}}$ in Eq. (15) becomes imaginary, and then the circular orbit is not allowed. It is also true for the extremal charged BTZ black hole.

FIGURES

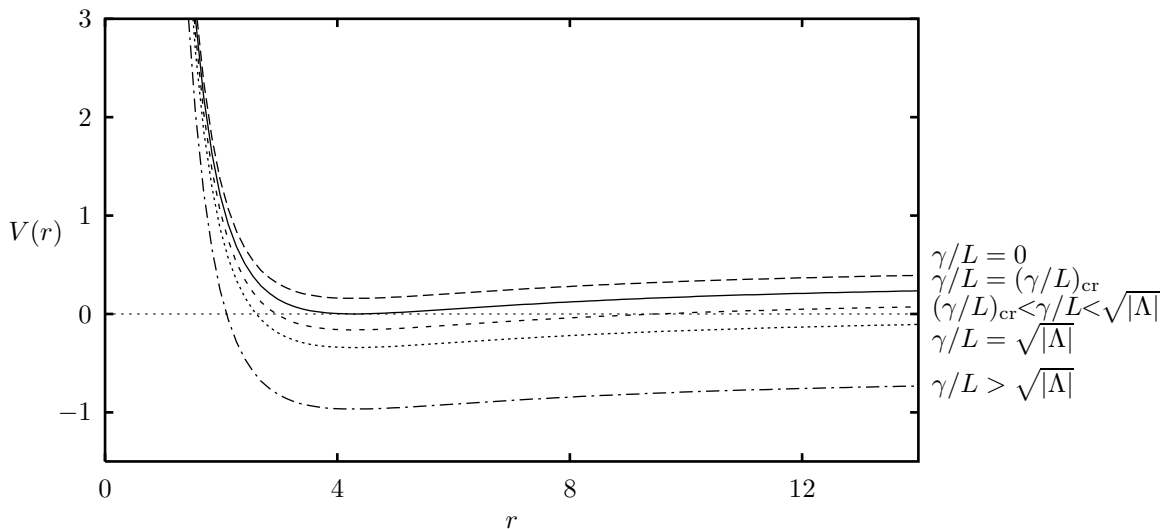


FIG. 1. The schematic shapes of effective potential $V(r)$ for various values of γ/L when $M/|\Lambda| = -3$, $q^2/|\Lambda| = 1$, and $G = 1$. Since $M/|\Lambda| < (\pi q^2/2) [1 - \ln(4\pi G q^2/|\Lambda|)] = -3$, the corresponding metric does not have a horizon.

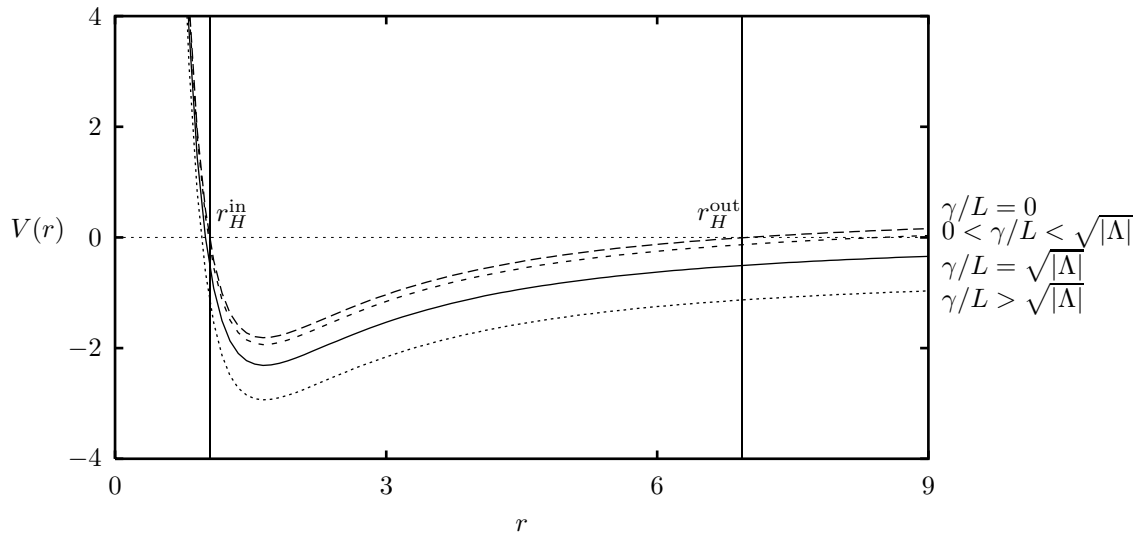


FIG. 2. The schematic shapes of effective potential $V(r)$ for various values of γ/L when $M/|\Lambda| = 0$, $q^2/|\Lambda| = 1$, and $G = 1$. Since $M/|\Lambda| > (\pi q^2/2) [1 - \ln(4\pi G q^2/|\Lambda|)] = 0$, the corresponding metric has two horizons.

We have already mentioned that Eq. (14) becomes integrable when $\gamma/L = \sqrt{|\Lambda|}$. The explicit form of the integrable orbits is

$$r = \exp\left(2\pi Gq^2\theta^2 - \frac{M}{\pi q^2}\right), \quad (17)$$

and FIGs. 3 and 4 show an example. FIG. 4 shows representative trajectories which are changed by the mass parameter with a fixed charge, $q^2/|\Lambda| = 1$. All possible motions are spiral at the large scale (see Fig. 3-(a)). As $M/|\Lambda|$ becomes sufficiently large, the radius of inner horizon approaches zero and that of outer horizon goes to infinity. In this limit, mass parameter determines the black hole dominantly and the charge does not affect much. Therefore, it leads to the Schwarzschild type black hole. When the black hole mass converges to that of extremal black hole case, i.e., $M \rightarrow (\pi q^2/2) [1 - \ln(4\pi Gq^2/|\Lambda|)]$, the radii of inner and outer horizons are merged into one;

$$r_H^{\text{ext}} = \sqrt{\frac{4\pi Gq^2}{|\Lambda|}}.$$

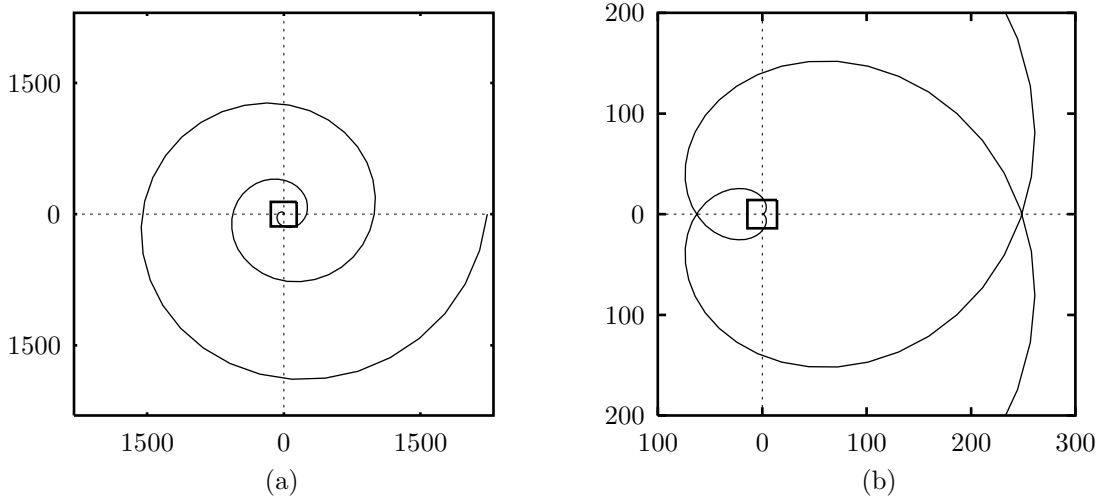


FIG. 3. (a). The photon trajectory falls into the black hole at large scale, and the region bounded by a small square is magnified in figure (b). (b). This figure shows incoming and outgoing photon trajectories, and the region bounded by a small square is displayed in FIG. 4. The coordinates of both figures are reduced to logarithmic scale, when $M/|\Lambda| = -3$, $q^2/|\Lambda| = 1$, $G = 1$, and $\gamma/L = \sqrt{|\Lambda|}$.

The perihelion of these analytically-obtained orbits in Eq. (17) is trivially obtained

$$r_{\text{ph}} = \exp\left(-\frac{M}{\pi q^2}\right), \quad (18)$$

and, for an extremal charged BTZ black hole, it becomes

$$r_{\text{ph}}^{\text{ext}} = \exp\left[\frac{1}{2}\left(\ln\frac{4\pi Gq^2}{|\Lambda|} - 1\right)\right]. \quad (19)$$

The perihelion of these analytically-obtained orbits in Eq. (17) is trivially obtained

$$r_{\text{ph}} = \exp\left(-\frac{M}{\pi q^2}\right), \quad (20)$$

and, for an extremal charged BTZ black hole, it becomes

$$r_{\text{ph}}^{\text{ext}} = \exp\left[\frac{1}{2}\left(\ln\frac{4\pi Gq^2}{|\Lambda|} - 1\right)\right]. \quad (21)$$

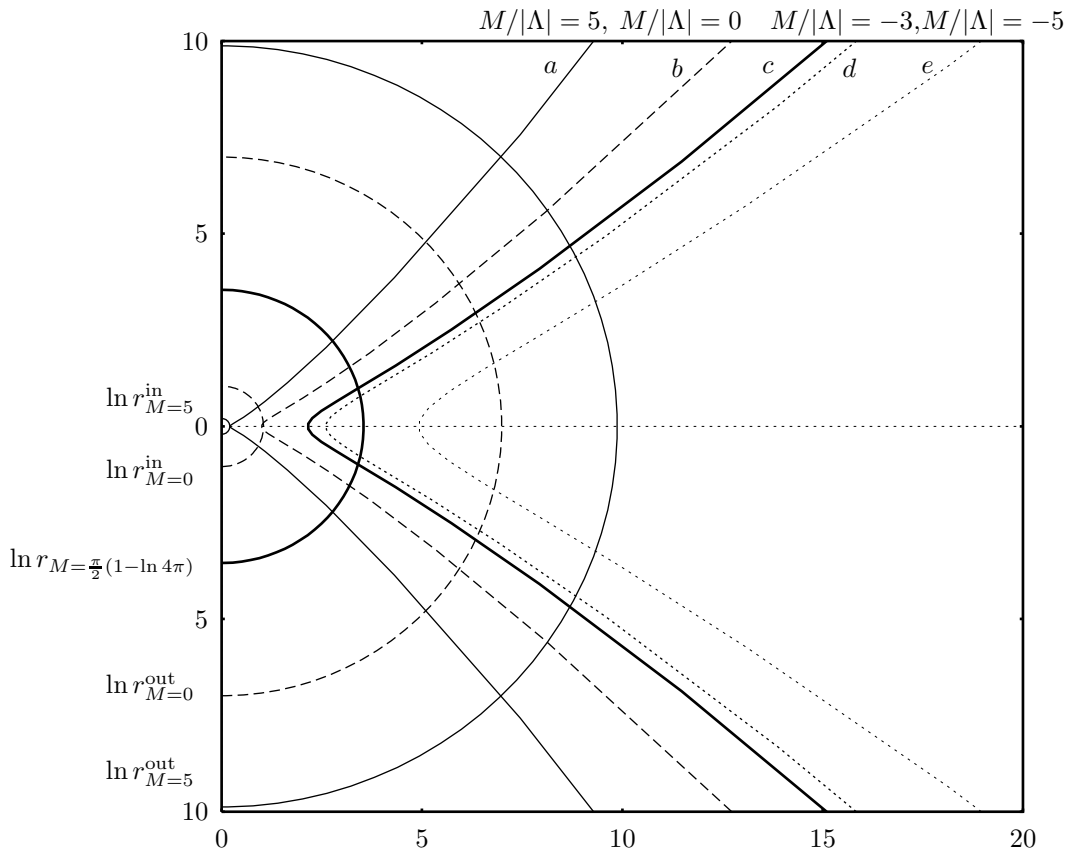


FIG. 4. This figure shows the photon trajectories when $M/|\Lambda|$ is changed. This figure is also reduced to logarithmic scale, when $q^2/|\Lambda| = 1$ and $G = 1$. The line (a) and (b) show the trajectories of charged BTZ black hole, the line (c) is that of extremal case of charged BTZ black hole, and the line (d) and (e) indicate the regular case. Each circles are horizons and the coordinate of this figure is also reduced to logarithmic scale.

As we mentioned previously, there remain two classes of solutions: (i) $(\gamma/L)_{\text{cr}} < \gamma/L < \sqrt{|\Lambda|}$ and (ii) $\gamma/L > \sqrt{|\Lambda|}$. When $\gamma/L \neq \sqrt{|\Lambda|}$, the orbit equation (14) is not integrable. Then the numerical analysis is a useful tool for those geodesic motions. For the first case $((\gamma/L)_{\text{cr}} < \gamma/L < \sqrt{|\Lambda|})$, all orbits are bounded between aphelion and perihelion. Two representative examples of elliptic geodesic motions are shown in FIG. 5. For the second case $(\gamma/L > \sqrt{|\Lambda|})$, FIGs. 1 and 2 show that there also exists perihelion but we cannot obtain analytically.

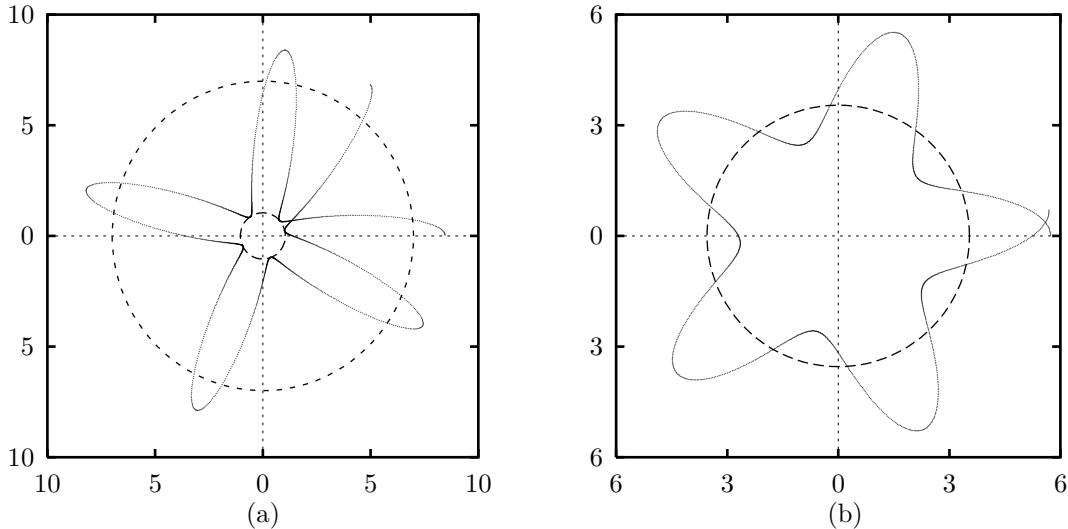


FIG. 5. (a). The figure shows a photon trajectory of charged BTZ black hole when $q^2/|\Lambda| = 1$, $M/|\Lambda| = 0$, $m = 0$, $L = 1$, and $\gamma = 0.5$. (b). The figure shows that of an extremal charged BTZ black hole when $q^2/|\Lambda| = 1$, $M/|\Lambda| = \frac{\pi}{2}(1 - \ln 4\pi)$, $m = 0$, $L = 1$, and $\gamma = 0.5$. The dashed circles are all horizons.

For the motions of a massive particle ($m = 1$), all allowed motions are bounded since the asymptotic structure of spacetime is not flat, but anti-de Sitter.

In the case of a massive test particle with zero angular momentum ($m = 1$ and $L = 0$), the effective potential becomes

$$V(r) = \frac{1}{2}B(r) - \frac{\gamma^2}{2}. \quad (22)$$

There is no allowed motion under the critical energy γ_{cr} . When the minimum value of the effective potential is zero, the critical energy of the test particle is computed;

$$\gamma_{\text{cr}} = \sqrt{4\pi Gq^2 \left(1 - \ln \frac{4\pi Gq^2}{|\Lambda|}\right) - 8GM}. \quad (23)$$

When $\gamma = \gamma_{\text{cr}}$, the test particle remains at rest. Above the critical energy, radial motion is an oscillation between perihelion and aphelion. For the black hole case, the motion of a test particle is also oscillating, but its range is restricted by the horizons.

In the case of a massive test particle with angular momentum ($m = 1$ and $L \neq 0$), the effective potential becomes

$$V(r) = \frac{1}{2}B(r) \left(\frac{L^2}{r^2} + 1\right) - \frac{\gamma^2}{2}. \quad (24)$$

FIG. 6 and FIG. 7 depict effective potentials for various values of γ : FIG. 6 corresponds to a regular spacetime and FIG. 7 a charged BTZ black hole.

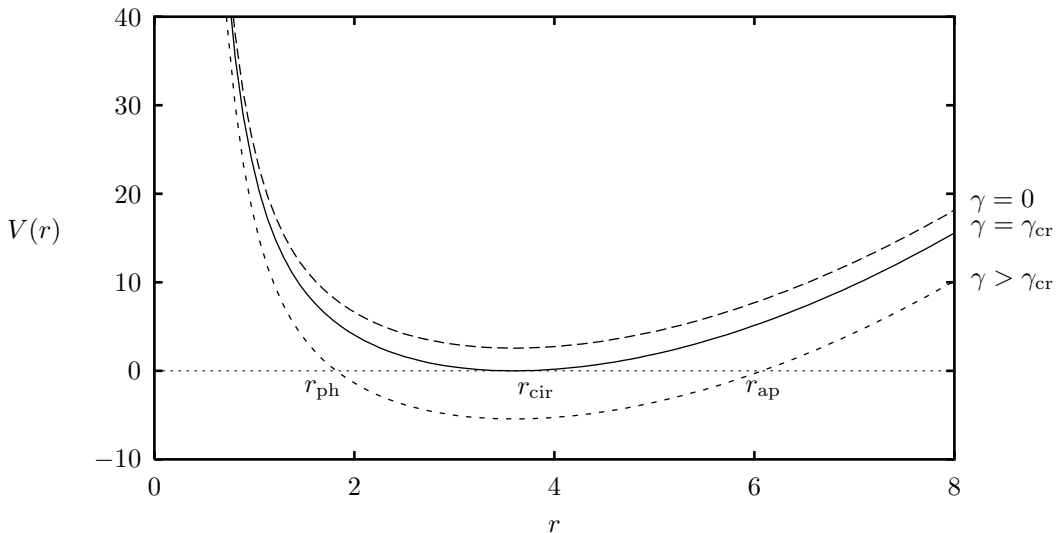


FIG. 6. The schematic shapes of effective potential $V(r)$ for various values of γ when $M/|\Lambda| = -3$, $q^2/|\Lambda| = 1$; $L = 1$, and $m = 1$. Since $M/|\Lambda| = -3$, the corresponding metric does not have a horizon.

For the regular case, the dashed line shows that the minimum of $V(r)$ is positive and then there is no allowed motion below this critical energy γ_{cr} . It is the same as that of the $L = 0$ case. When $\gamma = \gamma_{\text{cr}}$, the minimum of $V(r)$ is zero and then there exists a circular motion at $r = r_{\text{cir}}$ (see the solid line in FIG. 6). The effective potential given by the dotted line in FIG. 6 supports the elliptic motion with aphelion r_{ap} and perihelion r_{ph} . The effective potentials for a charged BTZ black hole are shown in FIG. 7. As shown in FIG. 7, the

motions outside the horizons are provided only when $\gamma > 0$. The unique allowed motion for the extremal charged BTZ black hole is the stopped motion at the degenerated horizon, which means eventually that no motion is allowed. Two examples of the trajectories of a massive test particle are described in FIG. 8.

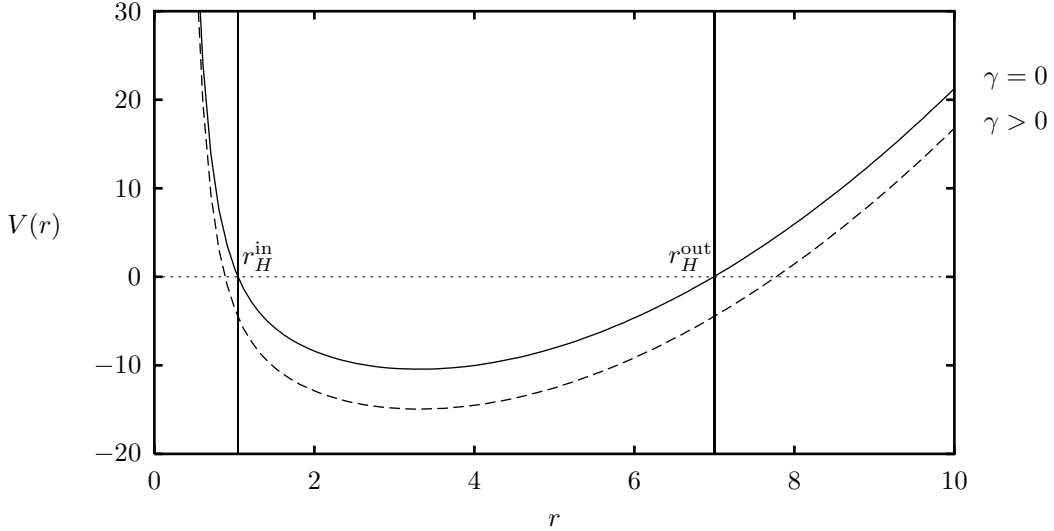


FIG. 7. The schematic shapes of effective potential $V(r)$ for various values of γ when $M/|\Lambda| = 0$, $q^2/|\Lambda| = 1$, $L = 1$, and $m = 1$. Since $M/|\Lambda| = 0$, the corresponding metric has two horizons.

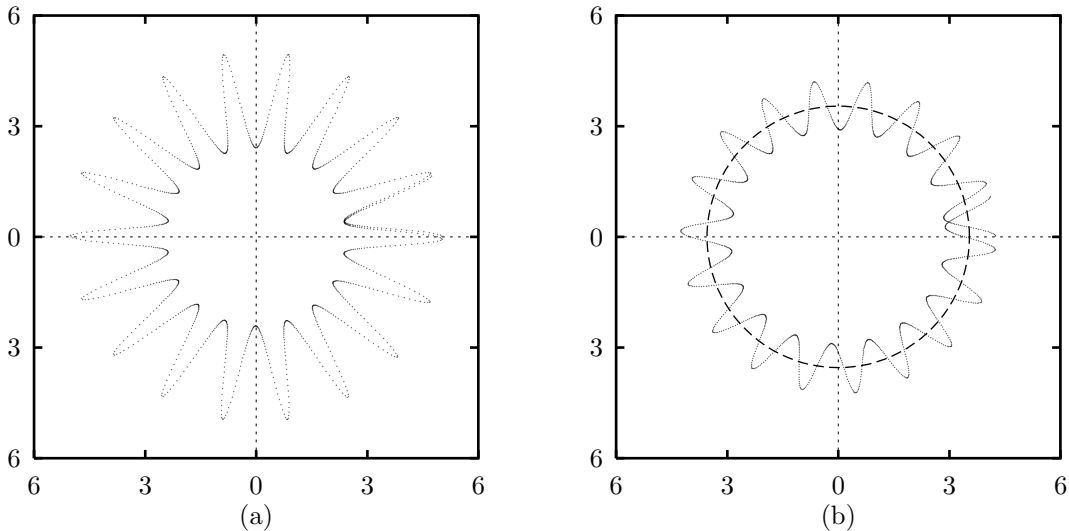


FIG. 8. (a). The figure shows a elliptic motion of regular case when $M/|\Lambda| = -3$ and $\gamma = 3$. (b). The figure shows that of extremal charged BTZ black hole when $M/|\Lambda| = (\pi/2) [1 - \ln(4\pi G/|\Lambda|)]$ and $\gamma = 1$. The other values are same for $q^2/|\Lambda| = 1$, $L = 1$, $m = 1$, and $G = 1$. The dashed circle in figure (b) indicates a extremal horizon.

III. CONCLUSION

In this paper we have studied the geodesic motions of charged BTZ black holes. We found a class of exact geodesic solutions of a massless test particle when the ratio of its energy and angular momentum is equal to the square root of the absolute value of a negative cosmological constant. The obtained geodesics describe the unbounded spiral motion. Though we have some exact geodesic motions, it seems impossible for us to extend our coordinates to Kruskal-Szekeres or Penrose diagram which provide a basis for further researches. We categorized the possible geodesic motions of massive and massless test particles as circular, elliptic, unbounded spiral, and unbounded motions. Several typical examples are analyzed by numerical works. Many works in various field, e.g., black hole thermodynamics, have been done for Schwarzschild- or Kerr-type BTZ black holes [4,5,10]. On the other hand, those researches have been limited in the case of charged BTZ black holes, that is different from that of $3 + 1$ dimensional Reissner-Nordström black holes. We hope that our simple work provides a building block to further researches about charged BTZ black holes and related topics.

ACKNOWLEDGMENTS

The authors would like to thank Yoonbai Kim for helpful discussions. This work was supported by KRF(1998-015-D00075) and KOSEF through Center for Theoretical Physics, SNU.

REFERENCES

- [1] M. Bañados, C. Teitelboim, and J. Zanelli, Phys. Rev. Lett. **69**, 1849 (1992); M. Bañados, C. Teitelboim, M. Henneaux, and J. Zanelli, Phys. Rev. D **48**, 1506 (1993).
- [2] S. Deser and R. Jackiw, Ann. Phys. (N.Y.) **153**, 405 (1984).
- [3] N. Kim, Y. Kim, and K. Kimm, Phys. Rev. D **56**, 8029 (1997); Y. Kim and S.-H. Moon, *ibid.* **58**, 105013 (1998); Y. Kim and K. Kimm, *ibid.* **58**, 107701 (1998).
- [4] S. Hyun, G. H. Lee, and J. H. Yee, Phys. Lett. B **322**, 182 (1994); K. Ghoroku and A. L. Larsen, Phys. Lett. B **328**, 28 (1994); I. Ichinose and Y. Satoh, Nucl. Phys. B **447**, 34 (1995); S. Carlip and C. Teitelboim, Phys. Rev. D **51**, 622 (1995); M. Natsuume, N. Sakai, and M. Sato, Mod. Phys. Lett. A **11**, 1467 (1996).
- [5] S. Carlip, Phys. Rev. D **51**, 632 (1995); M. Banados, T. Brotz, and M. Ortiz, Imperial/TP/97-98/23, DFTUZ 98105, hep-th/9802076.
- [6] J. Maldacena, Adv. Theor. Math. Phys. **2**, 231 (1998).
- [7] E. Witten, Adv. Theor. Math. Phys. **2**, 253 (1998).
- [8] C. Farina, J. Gamboa, and A. J Seguí-Santonja, Class. Quantum Grav. **10**, 193 (1993); N. Cruz, C. Martínez, and L. Peña, Class. Quantum Grav. **11**, 2731 (1994).
- [9] J. D. Brown and J. W. York, Phys. Rev. D **47**, 1407 (1993); J. D. Brown, J. Creighton, and R. B. Mann, *ibid.* **50**, 1040 (1994).
- [10] N. Kaloper, Phys. Rev. D **48**, 2598 (1993); G. T. Horowitz and A. A. Tseytlin, Phys. Rev. Lett. **73**, 3351 (1994).